

Developing *E. coli*-*E. coli* co-cultures to overcome barriers of heterologous tryptamine biosynthesis

Xiaonan Wang, Lizelle Policarpio, Dhara Prajapati, Zhenghong Li, Haoran Zhang*

Department of Chemical and Biochemical Engineering

Rutgers, The State University of New Jersey

98 Brett Rd, Piscataway, NJ 08854

* Corresponding author.

8 E-mail address: Haoran.Zhang@rutgers.edu

10

Abstract

11

12 Tryptamine is an alkaloid compound with demonstrated bioactivities and is also a precursor
13 molecule to many important hormones and neurotransmitters. The high efficiency biosynthesis of
14 tryptamine from inexpensive and renewable carbon substrates is of great research and application
15 significance. In the present study, a tryptamine biosynthesis pathway was established in a
16 metabolically engineered *E. coli*-*E. coli* co-culture. The upstream and downstream strains of the
17 co-culture were dedicated to tryptophan provision and conversion to tryptamine, respectively. The
18 constructed co-culture was cultivated using either glucose or glycerol as carbon source for de novo
19 production of tryptamine. The manipulation of the co-culture strains' inoculation ratio was adapted
20 to balance the biosynthetic strengths of the pathway modules for bioproduction optimization.
21 Moreover, a biosensor-assisted cell selection strategy was adapted to improve the pathway
22 intermediate tryptophan provision by the upstream strain, which further enhanced the tryptamine
23 biosynthesis. The resulting biosensor-assisted modular co-culture produced 194 mg/L tryptamine
24 with a yield of 0.02 g/g glucose using shake flask cultivation. The findings of this work
25 demonstrate that the biosensor-assisted modular co-culture engineering offers a new perspective
26 for conducting microbial biosynthesis.

27

28 **Keywords:** modular co-culture engineering, biosensor, *E. coli*, tryptamine, pathway
29 modularization

30

31

32 **1. Introduction**

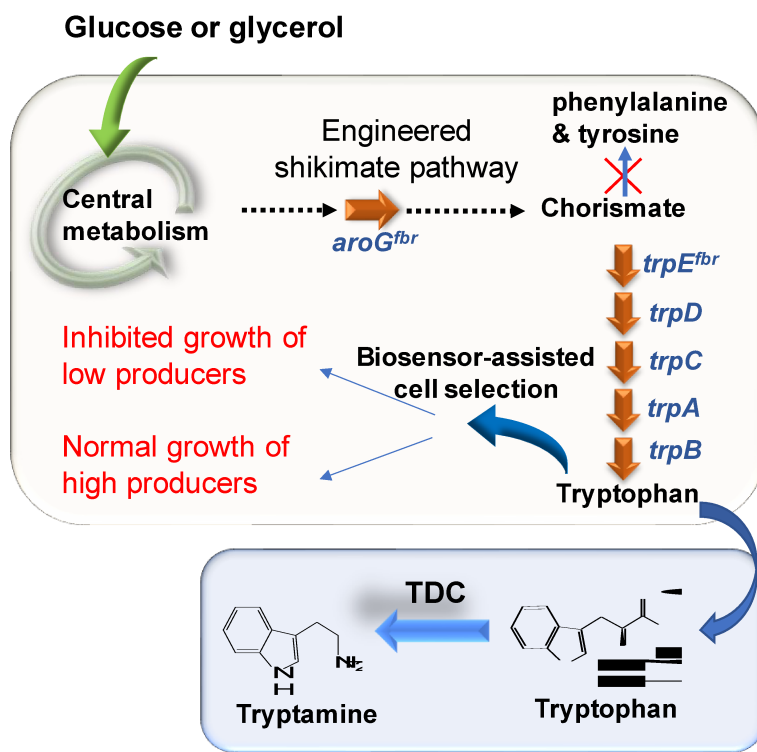
33 Tryptamine is a biogenic amine that belongs to the family of monoamine alkaloid.
34 Tryptamine is not only considered as a brain neurotransmitter by itself, but a precursor for making
35 many important bioactive molecules such as serotonin, melatonin, and substituted tryptamines
36 (Kang et al., 2007; Mahmood et al., 2010; Mousseau, 1993). Therefore, there has been consistent
37 interest for producing this valuable molecule with low cost and high efficiency. Tryptamine can
38 be biosynthesized from amino acid tryptophan by a tryptophan decarboxylase. As such, the
39 integration of tryptophan decarboxylation into the tryptophan biosynthesis pathway enables the de
40 *novo* production of tryptamine, as shown in Fig. 1. It has been reported that the expression of the
41 tryptophan decarboxylase in transgenic tobacco resulted in accumulation of tryptamine (Songstad
42 et al., 1990). For microbial biosynthesis, previous studies have established a heterologous pathway
43 in *E. coli* for biosynthesis of tryptamine and serotonin from glucose (Mora-Villalobos and Zeng,
44 2018; Park et al., 2011). Lee et al. further extended the pathway for producing tryptamine
45 derivatives such as N-hydroxycinnamoyl tryptamine in *E. coli* (Lee et al., 2017). However, so far,
46 no dedicated efforts have been made for *de novo* tryptamine biosynthesis and its optimization
47 using simple carbon substrate such as glucose and glycerol.

48 It is noteworthy that previous studies on microbial biosynthesis of tryptamine and its
49 derivatives employed the conventional mono-culture engineering strategy, i.e., utilization of the
50 culture containing one single metabolically engineered microbial strain. In recent years, modular
51 co-culture engineering has emerged as an innovative and effective approach for biosynthesis of a
52 wealth of value-added biochemicals (Chen et al., 2019; Jawed et al., 2019; Jones and Wang, 2018;
53 Roell et al., 2019; Zhang and Wang, 2016). In particular, the pathway modularization and
54 balancing in the context of co-cultures add a new dimension for microbial biosynthesis. A variety

55 of same-species co-cultures (e.g. *E. coli*-*E. coli* co-cultures) and multiple species co-cultures (e.g.
56 *E. coli*-*S. cerevisiae* co-cultures), have been successfully constructed to address the challenges for
57 biosynthesis performance enhancement. Meanwhile, new engineering strategies, such as using
58 poly-cultures consisting of three or more microbial strains, symbiotic growth of the co-culture
59 members, and co-culture mathematical modelling, been developed to extend the utility of the
60 modular co-culture engineering (Bayer et al., 2009; Jones et al., 2017; Li et al., 2019; Niehaus et
61 al., 2019). The accomplishments of the previous efforts offer strong incentive for using microbial
62 co-cultures for achieving efficient tryptamine bioproduction. In the present study, we
63 metabolically engineered and optimized an *E. coli*-*E. coli* co-culture for producing tryptamine
64 from renewable carbon substrates glucose and glycerol. In this co-culture system, the upstream
65 strain was constructed for producing the intermediate tryptophan, and the downstream strain was
66 engineered for converting tryptophan to the final product tryptamine using tryptophan
67 decarboxylase TDC (Fig. 1). Accordingly, the pathway balancing could be pursued by
68 manipulating the relative biosynthetic strengths for tryptophan provision and consumption, which
69 was conducted through adjusting the ratio between the upstream and downstream strains'
70 subpopulations.

71 In order to address the issue of insufficient pathway intermediate provision, a biosensor-
72 assisted cell selection approach was adapted for the constructed co-cultures. To this end, there
73 have been pioneering efforts using biosensors in metabolic engineering and synthetic biology
74 applications. For example, genetic and metabolic heterogeneity can lead to variations of
75 biosynthesis performance of the cells within a population. Several biosensors-assisted systems
76 have been developed and utilized to address this issue to serve biosynthesis enhancement. (Liu et
77 al., 2017; Rubjerg et al., 2018; Snoek et al., 2018; Wang et al., 2019; Xiao et al., 2016).

78 Specifically, a metabolite-responsive biosensor and a growth-regulation gene are integrated
 79 together, which provides regulation rules that promote the growth of cells producing high amounts
 80 of the target metabolite and inhibit the growth of the cells producing low amount of the target
 81 metabolite (Lv et al., 2019). In a recent study by our group, such a biosensor-assisted cell selection
 82 mechanism was integrated into microbial co-cultures to enhance the bioproduction of a commodity
 83 chemical phenol through improving the provision of pathway intermediates (Guo et al., 2019).



84

85 **Fig. 1** The co-culture design for biosynthesis of tryptamine. The upstream strain is responsible
 86 for producing tryptophan from simple substrate glucose or glycerol. The downstream strain is
 87 dedicated to converting tryptophan into tryptamine. The over-expressed pathway genes are
 88 indicated by solid arrows. Tryptophan decarboxylase (TDC) was expressed in the downstream
 89 strain. The biosensor-based selection systems were introduced into the upstream strain for
 90 enhancement of tryptophan provision.

91

92 Here, we extended the use of biosensor-assisted cell selection for facilitating the
93 biosynthesis of tryptamine in the context of engineered *E. coli*-*E. coli* co-cultures. Specifically,
94 two independent biosensor-assisted cell selection systems were recruited for enhancing the
95 tryptophan bioproduction in the upstream strain of the constructed co-culture system. The
96 biosensor of the first system employed the leader peptide gene *tnaC* of the *tnaCAB* operon which
97 senses tryptophan abundance and control gene expression through interaction with transcription
98 termination factor Rho. The tetracycline resistance gene *tetA* was used as the growth-regulating
99 component of this cell selection system. For such a *tnaC-tetA* system, high tryptophan
100 concentration switched on the *tetA* expression and thus enabled the growth the cell in the presence
101 of exogenous antibiotic tetracycline. The second system contained the *mtr* gene promoter and the
102 toxin gene *hipA*. High tryptophan concentration switched off the expression of the toxic expression
103 of the *hipA* gene and thus promoted cell growth. Our results showed that using these two systems,
104 the engineered co-cultures' tryptamine bioproduction production was improved significantly. It is
105 therefore demonstrated that biosensor-assisted modular co-culture engineering is an effective
106 strategy for enhancing heterologous tryptamine biosynthesis in *E. coli*.

107 **2. Materials and Methods**

108 **2.1 Plasmids and strains construction**

109 Strains and plasmids used in this work are listed in Table 1. Sequences of the primers used
110 in this study are listed in Supplementary Information. Tryptophan decarboxylase from
111 *Catharanthus roseus* TDC (GenBank accession no. J04521) was codon-optimized for *E. coli*
112 expression and synthesized by Bio basic Inc. Nucleotide sequences of *TDC* gene is provided in the
113 Supplementary Information. DNA purification and plasmids isolation used kits from Zymo

114 Research (Irvine, CA, USA). All restriction enzymes, DNA ligase, Q5 Master-mix enzymes and
115 Gibson assembly builder were purchased from New England Biolabs. Plasmid construction was
116 conducted using *E. coli* DH5 α (New England Biolabs) competent cells. All cloning procedures
117 were performed according to the manufacturer's protocols. Detail information for plasmid
118 construction is described as follows.

119 To construct plasmid pTS, three DNA fragments, including *tnaC* sequence with the
120 *tnaCAB* operon promoter PCR amplified from the *E. coli* K12 chromosome by primers Tnac-Gf
121 and Tnac-Gr, the *tetA* fragment PCR amplified from pBR322 plasmid by primers Tet-a-Gf and
122 Tet-a-Gr, and plasmid pET21c backbone digested with SphI/NotI, were assembled together using
123 the Gibson assembly kit (New England Biolabs). To construct plasmid pTC, the *tetA* gene with
124 the promoter was PCR amplified from pBR322 using primer Tet-f and Tet-r, digested with
125 NdeI/XhoI, and then ligated with plasmid pET21c treated with the same enzymes. To construct
126 plasmid pTY0, a DNA fragment containing the codon-optimized *TDC* gene was synthesized (Bio
127 Basic Inc. New York) (Park et al., 2011), digested by HindIII and XhoI, and ligated with the
128 plasmid pTE0 treated with the same restriction enzymes ([Wang et al., 2019](#)). To construct pTY1,
129 the *aroG^{br}* (*aroG* (Asp146Asn)) gene was PCR amplified from the *E. coli* P2H chromosome using
130 primer AroG-f and AroG-r, digested with BamHI/Sall, and ligated with pTY0 treated with the
131 same restriction enzymes ([Ganesan et al., 2017](#)). To construct pTY2, the *Ppdc- trpE^{br}* DNA
132 fragment was PCR amplified from a previously constructed plasmid pTE3-1 using primer CST-
133 trpE-f and CST-trpE-r (Wang et al., 2019), digested with SphI/SpeI, and then ligated with plasmid
134 pTY1 treated with SphI/XbaI. To construct pTY3, the *Ppdc-trpD-trpC* fragment was PCR
135 amplified from a previous constructed plasmid pTD2-1 using primer CST-TrpDC-f and CST-
136 TrpDC-r ([Wang et al., 2019](#)), digested with EcoNI/NdeI, and then ligated with pET21c plasmid

137 treated with the same restriction enzymes. To construct pTY4, a DNA fragment containing the
138 codon-optimized *TDC* gene was synthesized (Bio Basic Inc. New York), digested by NdeI/XhoI,
139 and ligated with the plasmid pET28a treated with the same restriction enzymes. To construct pTY5,
140 the *TDC* fragment was generated by NcoI/XhoI digestion of pTY4, which was then ligated with
141 plasmid pTY3 treated with the same restriction enzymes. To construct pTD3, the *Ppdc-trpDCBA*
142 fragment was generated by digestion of pTD2 by EcoNI/XhoI, which was then ligated with
143 pCDFDuet-1 plasmid treated with the same restriction enzymes.

144 **2.2 Medium and cultivation conditions**

145 Tryptamine biosynthesis in this study was performed using an MY medium. One liter of
146 MY medium contained 6.8 g of Na₂HPO₄, 3 g of KH₂PO₄, 1 g of NH₄Cl, 0.5 g of NaCl, 0.24 g of
147 MgSO₄, 0.5 g of yeast extract, 40 mg of tyrosine, 40 mg of phenylalanine, 5 g glucose, and trace
148 elements. The working concentrations of trace elements were 0.4 mg/L Na₂EDTA, 0.03 mg/L
149 H₃BO₃, 1 mg/L thiamine, 0.94 mg/L ZnCl₂, 0.5 mg/L CoCl₂, 0.38 mg/L CuCl₂, 1.6 mg/L MnCl₂,
150 3.77 mg/L CaCl₂, and 3.6 mg/L FeCl₂. For biosynthesis on glycerol, 5 g glycerol was used to
151 replace glucose. The working concentrations of antibiotics were 50 mg/L kanamycin, 34 mg/L
152 chloramphenicol, and 100 mg/L ampicillin. When needed, 10 mg/L tetracycline was used for the
153 biosensor-assisted cell selection.

154 Both *E. coli* mono-cultures and co-cultures were cultivated in 10 mL MY medium under
155 250 rpm at 30 °C. For mono-culture cultivation, 10 % (v/v) overnight LB culture of the desired *E.*
156 *coli* strains was inoculated into the MY medium with proper antibiotics and incubated at 37 °C for
157 8 h. The cells were then harvested by centrifugation and re-suspended in the fresh MY medium
158 with an initial OD₆₀₀ of 0.5. After 48 h cultivation, the culture samples were taken for HPLC
159 analysis. For *E. coli*–*E. coli* co-cultures, 10 % (v/v) overnight LB cultures of the desired *E. coli*

160 strains were cultivated in the MY medium as seed cultures, respectively. After 8 h growth at 37
161 °C, the upstream and downstream cell seed cultures were measured for cell density, harvested by
162 centrifugation, and inoculated into the MY medium containing appropriate antibiotics. The needed
163 volumes for individual seed cultures were calculated based on the desired inoculation ratios. The
164 initial OD₆₀₀ of the co-culture after inoculation was controlled at 0.5, followed by 48 h cultivation
165 at 30 °C.

166 For biosynthesis time profile analysis, seed cultures were grown in shake flasks containing
167 30 mL MY medium and cultivated at 37 °C for 12 h. The seed cultures of the upstream strains and
168 the downstream strains were then inoculated into 30 mL MY medium containing 10 g/L glucose.
169 The initial OD₆₀₀ of the co-culture after inoculation was controlled at 0.5 with the desired upstream:
170 downstream ratio, followed by 72 h cultivation in 250 mL shake flasks at 30 °C.

171 **2.3 Construction and characterization of tryptophan biosensor-assisted cell selection system**

172 The pTS plasmid containing the tryptophan biosensor-assisted selection system was
173 composed of the *tetA* gene fused downstream to the *tnaC* gene. The *tnaC* gene encodes the leading
174 sequence of the *tnaCAB* operon, whose expression was induced by tryptophan (Supplementary
175 Information) ([Gong and Yanofsky, 2001](#); [Yanofsky et al., 1991](#)).

176 Strain BLXS was constructed by introducing plasmid pTS into *E. coli* BL21(DE3). Strain
177 BLXC was used as a control strain for growth characterization. The *E. coli* strains were first
178 cultivated in the LB medium at 37 °C. The overnight culture was then centrifuged and re-
179 suspended in fresh MY medium containing 10 mg/L tetracycline. The initial OD₆₀₀ was kept at
180 0.5. Desired amounts of tryptophan were added to the culture to generate different working

181 concentrations. After cultivation under 250 rpm at 30 °C for 18 h, the cultures were subjected to
182 cell density analysis by measuring the light absorption at 600 nm.

183 **2.4 Quantification of tryptophan and tryptamine**

184 To quantify tryptophan and tryptamine, *E. coli* culture samples were centrifuged at 10,000
185 rpm for 5 min, and the supernatants were filtered through 0.45 mm PTFE membrane syringe filters.
186 10 µL filtered sample was injected into an AcclaimTM AmG C18 HPLC column controlled by a
187 Shimadzu HPLC system with a diode array detector set to a wavelength of 280 nm. The samples
188 were eluted using 97% solvent A (0.5 % acetic acid in HPLC water) and 3% solvent B (99.9 %
189 acetonitrile) running at a flow rate of 0.6 mL/min.

190 **2.5 Determination of co-culture population composition**

191 The determination of the co-culture population composition was conducted by the blue-
192 white colony counting method described in a previous report (Zhang et al., 2015b). 8 µL of the co-
193 culture sample was diluted 10⁶-fold and then spread onto an LB agar plate containing IPTG and
194 X-Gal. After 12 h of incubation at 37 °C, the upstream strains (BTP1 or BTS1) carrying the intact
195 *lacZ* gene generated blue colonies, while the downstream strain XYD containing the disrupted
196 *lacZ* gene generated white colonies. The numbers of the blue and white colonies on the plates were
197 counted for calculating the strain-to-strain ratio of the co-culture population.

198 **3. Results**

199 **3.1 Design and construction of the *E. coli*-*E. coli* co-culture for tryptamine de novo
200 biosynthesis**

201 In order to employ the modular co-culture engineering strategy for tryptamine biosynthesis,
202 we designed an *E. coli*-*E. coli* co-culture harboring the pathway leading from carbon substrate
203 glucose or glycerol to tryptamine. Specifically, there were two individually engineered *E. coli*
204 strains within the co-culture system. As shown in Fig. 1, the upstream strain was constructed for
205 tryptophan overproduction; the downstream strain was engineered for converting tryptophan to
206 tryptamine. Notably, the pathway intermediate tryptophan is known to be capable of move across
207 the cell membrane (Burkovski and Krämer, 2002), which enables the connection of the two
208 pathway modules accommodated by the two separate co-culture strains.

209 The upstream co-culture strain BTP1 was constructed in a previous study (Wang et al.,
210 2019). This strain contained two plasmids pTD2 and pTE3 for over-expression of the key
211 tryptophan pathway genes, including feedback control resistant DAHP synthase *aroG*^{fr}, feedback
212 control resistant anthranilate synthase subunit *trpE*^{fr}, anthranilate synthase subunit *trpD*,
213 tryptophan synthase subunit genes *trpA* and *trpB*, and indole-3-glycerol phosphate
214 synthase/phosphoribosylanthranilate isomerase *trpC* (Table 1). *E. coli* XL10-Gold was used as the
215 host strain for downstream conversion from tryptophan to tryptamine, as this strain showed
216 outstanding performance for biosynthesis of another aromatic molecule 3-amino-benzoic acid
217 using an engineered co-culture (Zhang and Stephanopoulos, 2016). The gene *TDC* encoding
218 tryptophan decarboxylase derived from *Catharanthus roseus* was codon-optimized and introduced
219 into *E. coli* XL10-Gold to yield the downstream co-culture strain XYD.

220 **3.2 Tryptamine bioproduction by an *E. coli*-*E. coli* co-culture without cell selection systems**

221 The engineered tryptophan over-producing strain BTP1 and the tryptophan-to-tryptamine
222 conversion strain XYD were co-cultured in one consolidated culture for de novo tryptamine
223 bioproduction on 5 g/L glucose or glycerol. The inoculum ratio between the upstream and

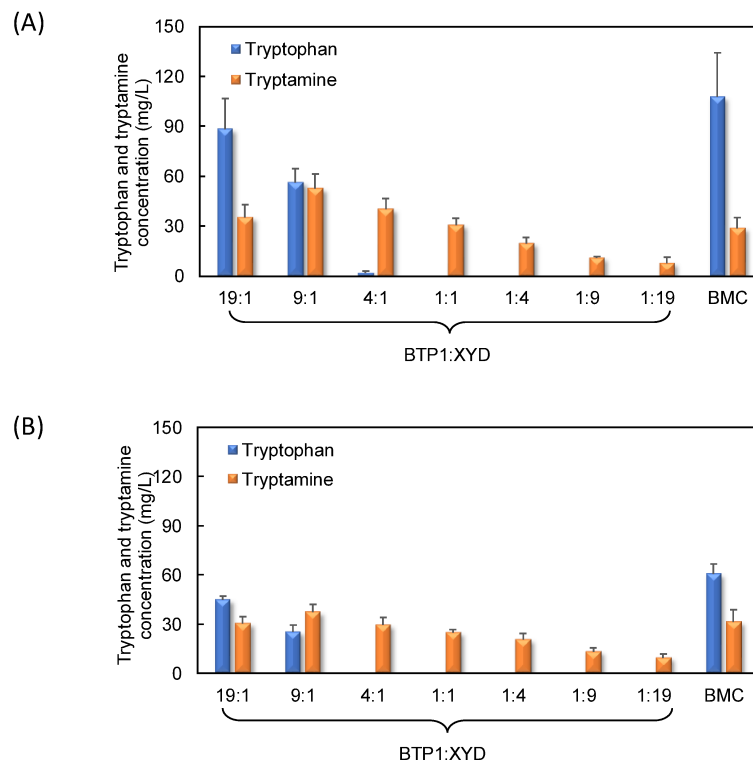
224 downstream co-culture strains was optimized to balance the biosynthesis capabilities of the
225 corresponding pathway modules. The mono-culture control strain BMC was constructed by
226 introducing the whole tryptamine biosynthesis pathway into the upstream strain (Table 1). Another
227 potential mono-culture control strain would be the downstream strain containing the whole
228 tryptamine biosynthesis pathway. However, this strain was not constructed and used in this study,
229 because the downstream strain was a poor host for producing tryptophan (Supplementary
230 Information Fig. S1).

231 For the tryptamine bioproduction on glucose, the constructed mono-culture and co-culture
232 systems were cultivated under the same condition for comparison. As shown in Fig. 2A, the
233 tryptamine biosynthesis by the engineered co-culture varied significantly with the inoculum ratio.
234 Excessive inoculation of the upstream strain BTP1 resulted in overly high tryptophan supply,
235 which led to relatively small sub-population of the downstream strain and insufficient tryptophan-
236 to-tryptamine bioconversion. On the contrary, when the downstream strain was inoculated with
237 high ratio, the supply of tryptophan from the upstream strain was diminished. Due to these two
238 effects, the optimal tryptamine production was achieved at the ratio of 9:1, under which the
239 tryptamine bioproduction reached 53 mg/L, although there was also accumulation of 56 mg/L
240 tryptophan. In comparison, the mono-culture control strains BMC produced 30 mg/L tryptamine
241 under the same conditions.

242 The constructed co-culture also showed desired tryptamine production when 5 g/L glycerol
243 was used as the carbon source. As shown in Fig. 2B, the final tryptamine concentration varied over
244 a wide range of the co-culture strains' inoculation ratio. The highest tryptamine production of 37
245 mg/L was achieved at the inoculation ratio of 9:1, which is the same with the optimal inoculation
246 rate for the biosynthesis on glucose. In comparison, the mono-culture control strains BMC

247 produced 32 mg/L tryptamine. Overall, the co-culture's tryptamine production on glucose was
248 higher than on glycerol, suggesting that glucose is a better carbon source for the tryptamine
249 bioproduction by the co-culture.

250



251

252 **Fig. 2** Tryptamine bioproduction by utilization of the BMC mono-culture and BTP1:XYD co-
253 culture inoculated at different ratios using (A) glucose and (B) glycerol as the carbon substrate.

254

255 It should be also noted that there was significant tryptophan accumulation in the mono-
256 culture control grown on both glucose and glycerol. In contrast, almost no tryptophan
257 accumulation was observed in the constructed co-culture at most of the inoculum ratios, indicating
258 that the constructed co-cultures had robust tryptophan-to-tryptamine conversion capability largely

259 due to the reduced metabolic burden on the downstream strain. In the meantime, this situation
260 suggested that the upstream supply of tryptophan was the limiting factor of the overall tryptamine
261 production in the co-cultures.

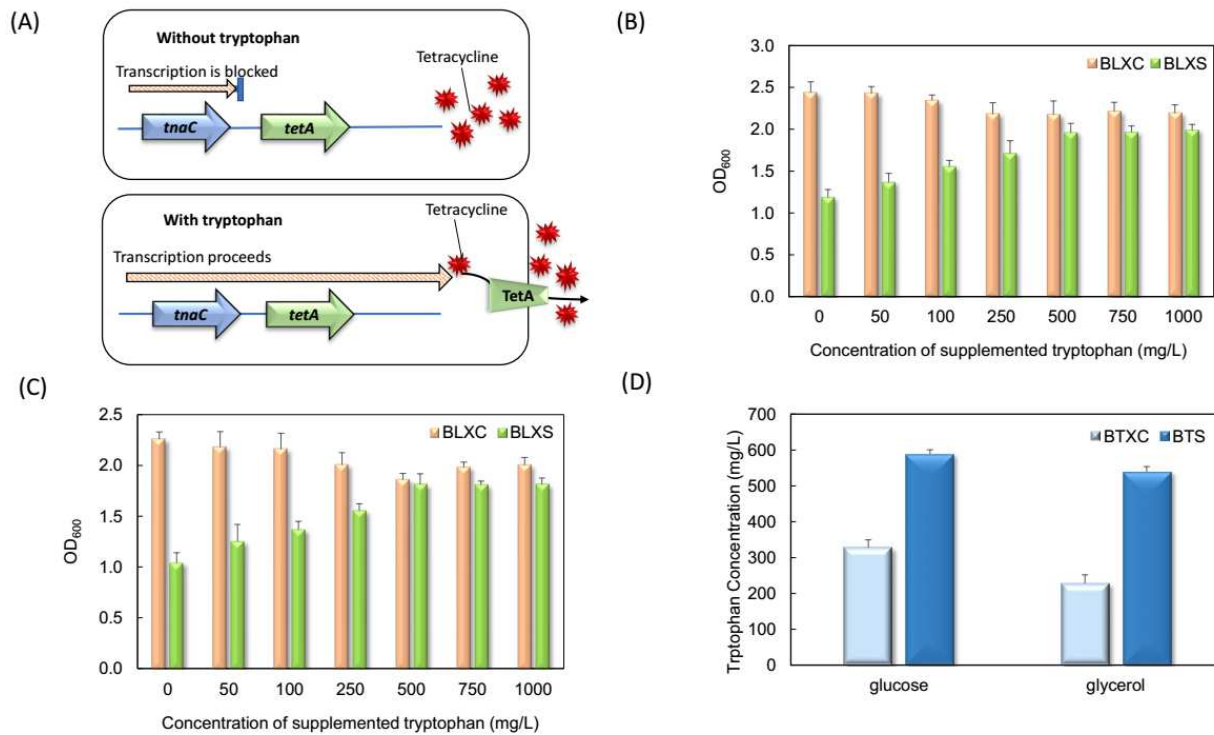
262 **3.3 Construction and characterization of the cell selection systems**

263 In order to improve the tryptophan supply and tryptamine production, two different
264 biosensor-assisted cell selection systems were introduced in the upstream strain, respectively. Each
265 cell selection system comprised a tryptophan-responsive biosensor and a growth-regulating gene,
266 as reported by previous studies (Wang et al., 2019; Xiao et al., 2016). Depending on the tryptophan
267 concentration, expression of the growth-regulating gene was up- or down-regulated. As a result,
268 the growth of the high tryptophan-producing cells was promoted, while the growth of low
269 tryptophan-producing cells was inhibited, as shown in Fig. 1. Therefore, the upstream strain's
270 population was dominated by the high tryptophan-producing cell and the overall tryptophan
271 production performance was enhanced.

272 For the first cell selection system, we used *E. coli tnaCAB* operon's leader peptide gene
273 *tnaC* to control the tetracycline resistance gene *tetA* expression (Fig. 3A). The strain harboring this
274 cell selection system was first characterized for growth regulation in response to varying
275 tryptophan concentrations. Specifically, *E. coli* BLXC and BLXS, two strains without and with
276 the *tnaC-tetA* cell selection system, were cultivated in the MY medium with 10 mg/L tetracycline.
277 As shown in Fig. 3B, BLXC's growth showed slight decrease with the increase of the exogenous
278 tryptophan concentration, possibly due to the cell toxicity associated with high tryptophan
279 concentration. The growth of BLXS, however, showed clear dependence on the tryptophan
280 concentration as expected: low tryptophan concentration inhibited the growth, whereas high
281 tryptophan concentration promoted the growth. In addition, BLXC and BLXS growth comparison

282 on glycerol demonstrated similar trend (Fig. 3C). These results indicate that the *tnaC-tetA* cell
 283 selection system has the desired tryptophan-sensing and cell growth regulation functions.

284



285

286 **Fig. 3** Construction and characterization of the *tnaC-tetA* cell selection system. (A) Scheme of
 287 the *tnaC-tetA* cell selectin mechanism. The presence of tryptophan decides whether the *tetA* gene
 288 can be expressed to resist the antibiotic tetracycline. (B) and (C) Growth behaviors of *E. coli* BLXS
 289 harboring the *tnaC-tetA* system on glucose and glycerol, respectively. 10 mg/L tetracycline and
 290 varying concentrations of tryptophan was added to the medium in both cases. *E. coli* BLXC was a
 291 control strain without the cell selection system. (D) Comparison of tryptophan biosynthesis
 292 between BTXC and BTS using glucose and glycerol as the carbon substrates.

293

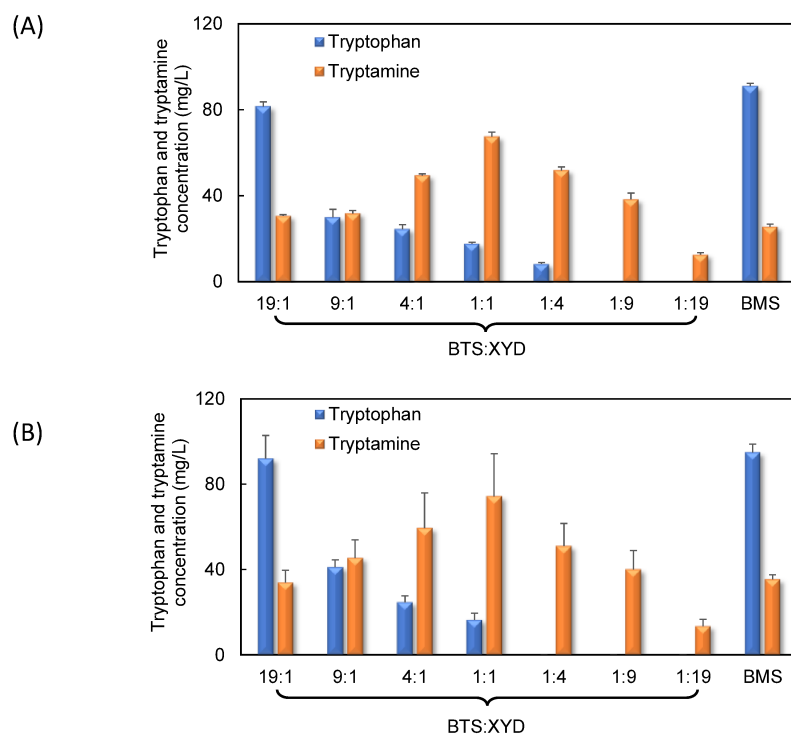
294 Next, the tryptophan production capability of the strain BTS harboring the *tnaC-tetA*
295 system was investigated. As shown in Fig. 3D, when 5 g/L glucose was used as the carbon source,
296 tryptophan production by BTS reached 588 mg/L, 80% higher than the control strain BTXC. The
297 tryptophan production on glycerol was also improved from 228 to 539 mg/L. The significant
298 production improvement on both glucose and glycerol demonstrate effectiveness of the *tnaC-tetA*
299 cell selection system.

300 For the second cell selection system, we recruited a tryptophan-responsive promoter
301 derived from the *E. coli* *mtr* gene to control the expression of the toxin *hipA* gene via the
302 tryptophan-binding protein TrpR. Notably, different from the first cell selection system, the
303 biosensor of this system is an off-switch that downregulates gene expression with high tryptophan
304 production. The *mtr-hipA* system had been previously characterized and showed strong effect for
305 improving tryptophan over-production in *E. coli* (Wang et al., 2019).

306 **3.4 Enhancing the tryptamine bioproduction using the *tnaC-tetA* system**

307 Based on the constructed *tnaC-tetA* cell selection system, a new upstream strain BTS was
308 developed and co-cultivated with the downstream strain XYD for the tryptamine biosynthesis. Fig.
309 4A shows the profile of tryptamine bioproduction on glucose. The highest tryptamine
310 concentration reached 67 mg/L, 26 % higher than the co-culture without the cell selection system.
311 The optimal inoculation ratio also shifted from 9:1 to 1:1, indicating that the application of the cell
312 selection strategy improved the tryptophan supply and reduced the need of high upstream strain
313 inoculation ratio. This was further confirmed by the appearance of tryptophan accumulation at the
314 inoculation ratio of 4:1, 1:1 and 1:4. A mono-culture control strain BMS was also constructed to
315 harbor the whole tryptamine pathway as well as the cell selection system. It was found that the cell
316 selection strategy did not improve the tryptamine production in this strain, compared with strain

317 BMC without the *tnaC-tetA* system. This finding is in good agreement with our previous study
 318 (Guo et al., 2019) and suggests that the use of cell selection mechanism in mono-culture resulted
 319 in selection of cells with high tryptophan accumulation but not high tryptamine production. This
 320 situation highlights the unique advantage of using biosensor-assisted cell selection in co-cultures
 321 over mono-cultures.



322
 323 **Fig. 4** Tryptamine bioproduction using the *tnaC-tetA* biosensor-assisted cell selection system. (A)
 324 glucose and (B) glycerol were used as the carbon substrates for tryptamine bioproduction by the
 325 BMS mono-culture and BTS:XYD co-culture inoculated at different ratios.

326
 327 The BTS:XYD co-culture was also used for tryptamine production on glycerol. As shown
 328 in Fig. 4B, 74 mg/L tryptamine was produced from 5 g/L glycerol at the optimal inoculation ratio

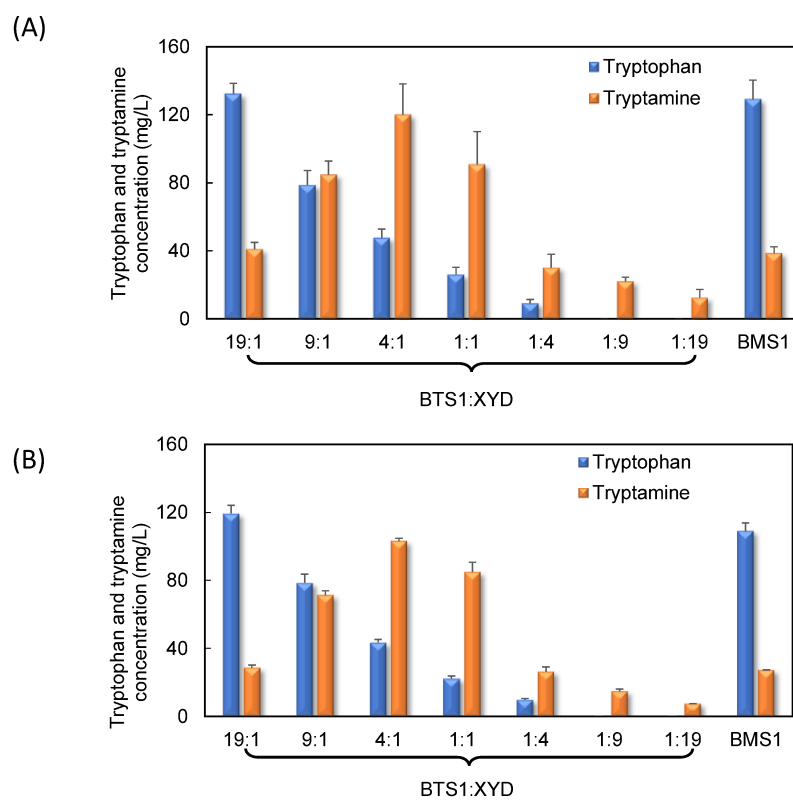
329 of 1:1. Such production was 2-fold higher than the co-culture without the cell selection system.
330 Moreover, the tryptophan supply was found to be enhanced in this production system, as evidenced
331 by the improved tryptophan accumulation and shifted optimal inoculation ratio. In comparison,
332 the mono-culture control strain BMS only produced 35 mg/L tryptamine under the same condition.

333 **3.5 Enhancing the tryptamine bioproduction using the *mtr-hipA* cell selection system**

334 In addition to the *tnaC-tetA* cell selection system, this study also explored the use of the
335 previously constructed *mtr-hipA* cell selection system (Wang et al., 2019). The corresponding co-
336 culture BTS1:XYD was used for de novo tryptamine bioproduction on glucose and glycerol. As
337 shown in Fig. 5A, the tryptamine production on glucose was significantly improved to 120 mg/L
338 at the optimal ratio of 4:1. This production is 79% higher than that of the co-cultures using the
339 *tnaC-tetA* cell selection system, suggesting that the *mtr-hipA* system is more robust for enhancing
340 the overall tryptamine biosynthesis performance. In fact, our previous study has shown that the
341 recruitment of the *E. coli* toxin system as the growth regulator resulted in higher bioproduction
342 performance than using the *tetA* gene (Wang et al., 2019). In the present study, it was further
343 confirmed that using toxin as the regulator is a robust method to improve the biosensor-targeted
344 metabolite biosynthesis. It should be noted, however, that the difference of binding affinity of
345 tryptophan with TrpR sensor protein of the toxin system and *tnaC* control element of the *tetA*
346 system could also contribute to the selection efficiency difference and bioproduction performance
347 variation. On the other hand, the BMS1 mono-culture control strains only produced 39 mg/L
348 tryptamine. This is consistent with the previous finding that the introduction of the cell selection
349 system into a mono-culture did not significantly improve the tryptamine production.

350 As shown in Fig. 5B, the tryptamine production on glycerol was also considerably
351 improved using the BTS1:XYD co-culture. At the optimal inoculation ratio of 4:1, the co-culture

352 produced 103 mg/L tryptamine from 5 g/L glycerol, which is 39% higher than the BTS:XYD co-
 353 culture using the *tnaC-tetA* system and 2.8-fold higher than the BTP1:XYD co-culture without the
 354 biosensor. The BMS1 mono-culture control strain only produced 27 mg/L tryptamine. The
 355 experimental results above clearly demonstrate that the recruitment of the *mtr-hipA* cell selection
 356 system is an effective strategy for enhancing the co-culture's capability for producing tryptamine
 357 on both glucose and glycerol.



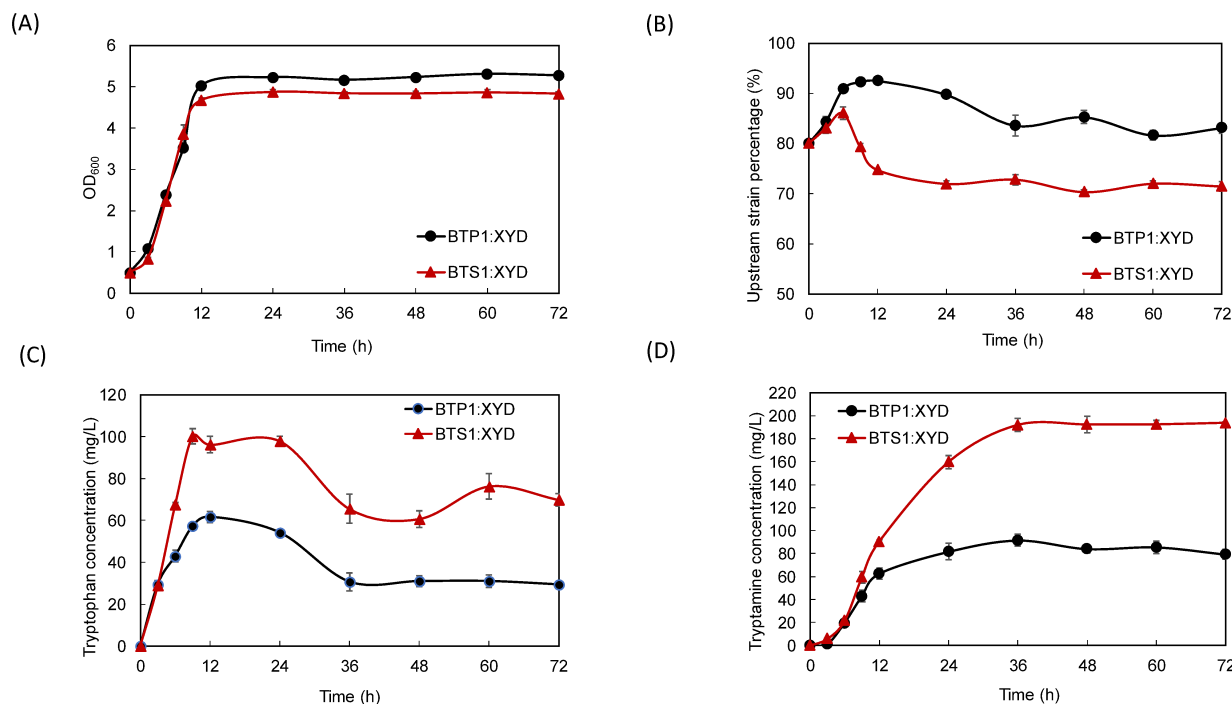
358

359 **Fig. 5** Tryptamine bioproduction using the *mtr-hipA* biosensor-assisted cell selection system. (A)
 360 glucose and (B) glycerol were used as the carbon substrates for tryptamine bioproduction by the
 361 BMS1 mono-culture and BTS1:XYD co-culture inoculated at different ratios.

362

363 3.6 Characterization of the co-culture biosynthesis behavior

364 In an effort to characterize the dynamic tryptamine biosynthesis behavior, the engineered
 365 BTS1:XYD co-culture (with the biosensor) and BTP1:XYD control co-culture (without the
 366 biosensor) were grown in shake flasks containing 10 g/L glucose at the inoculum ratio of 4:1. The
 367 overall culture cell density, strain-to-strain ratio, and pathway metabolite concentrations were
 368 analyzed throughout the cultivation. As shown in Fig. 6A, the growth of the co-culture systems
 369 followed the typical pattern of a batch culture. After the exponential phase between 3 and 12 h,
 370 the highest cell density was stabilized at $OD_{600} \approx 5.2$ for the control co-culture and $OD_{600} \approx 4.8$ for
 371 the BTS1:XYD co-culture with the biosensor. Notably, the BTS1:XYD co-culture's cell density
 372 was lower than the control co-culture, indicating that the *hipA*-based cell selection system inhibited
 373 the growth of the low-performing cells of the upstream strain and thus reduced the overall co-
 374 culture growth.



375
 376 **Fig. 6** Shake flask cultivation of the BTP1:XYD and BTS1:XYD co-cultures for the tryptamine
 377 bioproduction. Time profiles of (A) overall co-culture cell density, (B) upstream strain percentage,

378 (C) accumulation of the pathway intermediate tryptophan and (D) concentration of tryptamine
379 were derived from triplicate shake flask runs. Error bars represent standard errors of the
380 experimental results.

381

382 The time profiles of the upstream strains to downstream strain subpopulation ratio were
383 analyzed using a blue-white colony counting method (Zhang et al., 2015b). For the BTP1:XYD
384 co-culture, the percentage of BTP1 changed from 80% to 93% within 12 h and decreased to 83%
385 towards the end of the cultivation. This trend shows that the co-growth relationship between the
386 co-culture strains is a dynamic and fluctuating process. Interestingly, for the BTS1:XYD co-
387 culture, the percentage of BTS1 increased from 80% (0 h) to 86% (6 h), then decreased to 75%
388 (12 h) and lastly plateaued at 72% for the rest of the cultivation period. This sharp decline starting
389 from 6 h is considered to be due to the growth inhibition of the upstream strain's low-performing
390 cells resulted from the *mtr-hipA* cell selection system.

391 As shown in Fig. 6D, the co-culture BTS1:XYD was found to produce a considerably
392 higher amount of tryptamine than the control co-culture BTP1:XYD. The concentration of the
393 tryptamine in BTS1:XYD started to increase 3 h after the inoculation and plateaued at around 192
394 mg/L after 36 h; whereas the control group's tryptamine biosynthesis peaked at around 91 mg/L
395 at 36 h. In the meantime, it was found that the pathway intermediate tryptophan was accumulated
396 along with the co-culture growth (Fig. 6C). For BTP1:XYD, it was observed that tryptophan was
397 accumulated to around 62 mg/L at 12 h, decreased to 31 mg/L at 36 h and stabilized at this level
398 toward the end of cultivation. The tryptophan concentration was kept at a relatively low level at
399 most of the cultivation period, indicating that the insufficient intermediate supply limited the
400 production of tryptamine. In comparison, for BTS1:XYD, the tryptophan accumulation reached

401 100 mg/L at 9 h, decreased to 65 mg/L at 36 h and fluctuated around this level for the remaining
402 period of the cultivation. The accumulation of the pathway intermediate tryptophan was due to the
403 low subpopulation percentage of the downstream strain (less than 20%) shown in Fig. 6B.
404 Interestingly, the tryptamine production and tryptophan accumulation difference between the two
405 co-cultures both started to occur at around 6-12 h (Fig. 6C and D), suggesting that the enhancement
406 of tryptophan provision by the *mtr-hipA* based selection system took effect in the mid exponential
407 growth phase. This finding is consistent with the upstream strain percentage change at 6 h
408 discussed above.

409 Overall, the characterization of the BTS1:XYD co-culture biosynthesis showed that the
410 upstream strain occupied the majority of the co-culture population throughout the cultivation and
411 produce a sufficient amount of tryptophan for the conversion to tryptamine. On the other hand, the
412 downstream strain possessed strong biosynthetic capability that allowed it to complete effective
413 tryptophan to tryptamine conversion at a relatively low sub-population. The overall yield of the
414 tryptamine production of BTS1:XYD on glucose in shake flask was 0.02 g/g glucose. The
415 tryptamine production was mostly achieved within 36 h under the adapted cultivation condition.

416 **4. Discussion**

417 Tryptamine heterologous biosynthesis is of great research interest for improving this
418 compound's availability and facilitating the production of tryptamine derivatives with recognized
419 values. This study utilized the emerging modular engineering approach for reconstituting the
420 tryptamine biosynthesis pathway in the context of an *E. coli*-*E. coli* co-culture. Several engineering
421 strategies were applied for co-culture biosynthesis optimization. First, the inoculum ratios between
422 the upstream and downstream co-culture strains were varied to balance the biosynthetic
423 capabilities of the corresponding pathway modules. In fact, this strategy has been widely used in

424 previous studies for pathway balancing and bioproduction optimization in engineered co-cultures
425 (Chen et al., 2019; Jawed et al., 2019; Jones and Wang, 2018; Roell et al., 2019; Zhang and Wang,
426 2016). It should be noted that, even for the co-cultures composed of same-species strains, the
427 constituent strains often had quite different growth and biosynthesis behaviors. As a result, the
428 relative strain-to-strain ratio needs to be fine-tuned by varying the inoculum ratio. For this study,
429 it was found that the inoculum ratio indeed played a critical role in determining the bioproduction
430 performance. The optimal production was achieved at the inoculation ratio of 9:1, suggesting that
431 the biosynthesis capability of the upstream strain was at disadvantage and needed to be
432 compensated by high inoculum at the beginning of cultivation.

433 To further increase the supply of tryptophan for tryptamine production, we recruited two
434 cell selection mechanisms to select for tryptophan high-producing cells of the co-culture's
435 upstream strain. These cell selection mechanisms removed low performing cells from the
436 microbial population and have been verified to be an effective approach for target product
437 biosynthesis enhancement in the context of mono-culture (Lv et al., 2019; Rubjerg et al., 2018;
438 Wang et al., 2019; Xiao et al., 2016). In this study, it was shown that the *E. coli* toxin-based
439 selection system was more effective than antibiotic-based selection system for tryptamine
440 production improvement. In addition, the toxin-based selection system is straightforward to
441 implement in the co-culture, as it does not require any additional modification of the downstream
442 strain, such as introduction of new antibiotic resistance for compatible growth with the upstream
443 strain carrying the antibiotic-based cell selection system, which minimizes the impact on the
444 downstream strain's growth. On the other hand, such a cell selection strategy is challenging to
445 make positive impact in the mono-culture. In fact, for the mono-culture, the employment of the
446 cell selection mechanism using a tryptophan biosensor resulted in selection of the cells with high

447 tryptophan accumulation, whereas the conversion from tryptophan to tryptamine was not promoted
448 by the cell selection mechanism. This is supported by comparison of the tryptophan and tryptamine
449 production by strains BMC2 ad BMS without and with the *tnaC-tetA* system. As shown in Fig. S2,
450 BMS showed higher tryptophan accumulation capability but the same tryptamine production level
451 with BMC2 on both glucose and glycerol, confirming that when used in the context of mono-
452 culture, the cell selection system was mainly devoted to select for the cells with better tryptophan
453 accumulation, but not better tryptamine production. In contrast, the application of the cell selection
454 mechanism in the context of a rationally designed co-culture overcomes this issue, as the modular
455 nature of the co-culture allows for physical segregation and independent engineering of the co-
456 culture strains such that establishment of the cell selection mechanism in the upstream strain does
457 not reduce downstream strain's biosynthetic capability. As such, our results highlight the
458 outstanding advantages of integration of biosensor into co-cultures over into mono-cultures.

459 Glycerol is an important byproduct of the biodiesel industry and a renewable carbon
460 material with high abundance. Glycerol's utilization as carbon source for microbial biosynthesis
461 has attracting increasing research interest ([Clomburg and Gonzalez, 2013](#); [Mattam et al., 2013](#);
462 [Pradima and Kulkarni, 2017](#)). There have been efforts using modular co-culture engineering to
463 convert glycerol to important biochemical products, such as *cis,cis*-muconic acid and 3-
464 hydroxybenzoic acid ([Zhang et al., 2015a](#); [Zhou et al., 2019](#)). In this study, we confirmed that
465 glycerol can be used to produce tryptamine using the engineered co-culture, although the
466 production performance is lower than using glucose as the substrate. Also, it was found that the
467 integration of the designed cell selection system in the co-culture also improved the tryptamine
468 biosynthesis on glycerol. This result, together with the bioproduction improvement on glucose,

469 suggested that biosensor-assisted co-cultures can be more broadly used for biosynthesis using
470 other renewable carbon substrates, such as xylose and arabinose.

471 The shake flask cultivation achieved production of 194 mg/L tryptamine and 0.02 g/g
472 glucose production yield, which provides a robust platform for future biosynthesis of more
473 advanced end products, such as serotonin and melatonin. To this end, the required pathway
474 enzymes for making the target products can be conveniently expressed in the downstream strains
475 of the co-cultures without the undesired interference with the upstream pathway module which is
476 segregated in another strain. Therefore, the findings of this study and its potential utility for future
477 research demonstrate the potential and broad applicability of the modular co-culture engineering
478 in the future.

479

480 **Acknowledgement**

481 This material is based upon work supported in part by the National Science Foundation
482 under Grant No. 1706058. The authors are also grateful for the support by the startup research fund
483 provided by Rutgers, The State University of New Jersey. Zhenghong Li is a recipient of the CSC
484 Ph.D. fellowship.

485 **Conflict of interest**

486 The authors declare no financial or commercial conflict of interest.

487 **Table 1 Plasmids and strains used in this study.**

Plasmids	Description	Source
pET21c	T7 promoter, Amp ^R	Novagen

pBR322	Amp ^R , Tet ^R	Thermo Scientific
pET28a	T7 promoter, Kan ^R	Novagen
pCDFDuet-1	double T7 promoters, Strp ^R	Novagen
pACYCDuet-1	double T7 promoters, Cm ^R	Novagen
pTS	pET21c carrying tryptophan regulatory element (<i>tnaC</i> operon) and <i>tetA</i> gene, Amp ^R	This study
pTC	pET21c carrying the <i>tetA</i> gene, Amp ^R	This study
pTE0	pET28a carrying the <i>trpE^{fbr}</i> gene under the control of the T7 promoter, Kan ^R	(Wang et al., 2019)
pTE3-1	pUC57(Kan ^R) carrying the <i>trpE^{fbr}</i> , <i>pctV</i> and <i>shiA</i> genes under the control of the constitutive <i>Zymomonas mobilis</i> pyruvate decarboxylase promoter (P _{pdc}), Kan ^R	(Wang et al., 2019)
pTE3	pET28a carrying the <i>trpE^{fbr}</i> and <i>aroG^{fbr}</i> genes under the control of the constitutive <i>Zymomonas mobilis</i> pyruvate decarboxylase promoter (P _{pdc}), Kan ^R	(Wang et al., 2019)
pTY0	pET28a carrying the <i>trpE^{fbr}</i> and <i>TDC</i> genes under the control of the T7 promoter, Kan ^R	This study
pTY1	pET28a carrying the <i>trpE^{fbr}</i> , <i>aroG^{fbr}</i> and <i>TDC</i> genes under the control of the T7 promoter, Kan ^R	This study
pTY2	pET28a carrying the <i>trpE^{fbr}</i> , <i>aroG^{fbr}</i> and <i>TDC</i> genes under the control of the constitutive <i>Zymomonas mobilis</i> pyruvate decarboxylase promoter (P _{pdc}), Kan ^R	This study

pTD2-1	pUC57(Kan ^R) carrying the <i>trpD</i> and <i>trpC</i> genes under the control of the constitutive <i>Zymomonas mobilis</i> pyruvate decarboxylase promoter (P <i>pdc</i>) and <i>trpB</i> and <i>trpA</i> genes under the control of the T7 promoter, Kan ^R	(Wang et al., 2019)
pTY3	pET21c carrying the <i>trpD</i> and <i>trpC</i> genes under the control of the constitutive <i>Zymomonas mobilis</i> pyruvate decarboxylase promoter (P <i>pdc</i>), Amp ^R	This study
pTY4	pET28a carrying the <i>TDC</i> gene under the control of the T7 promoter, Kan ^R	This study
pTY5	pET21c carrying the <i>TDC</i> gene under the control of the constitutive <i>Zymomonas mobilis</i> pyruvate decarboxylase promoter (P <i>pdc</i>), Amp ^R	This study
pTD2	pACYCDuet-1 carrying the <i>trpD</i> , <i>trpC</i> , <i>trpB</i> and <i>trpA</i> genes under the control of the constitutive <i>Zymomonas mobilis</i> pyruvate decarboxylase promoter (P <i>pdc</i>), Cm ^R	(Wang et al., 2019)
pSE1	pET21c carrying the <i>hipA</i> gene under the control of the <i>mtr</i> promoter (P <i>mtr</i>), Amp ^R	(Wang et al., 2019)
pTD3	pCDFDuet-1 carrying the <i>trpD</i> , <i>trpC</i> , <i>trpB</i> and <i>trpA</i> genes under the control of the constitutive <i>Zymomonas mobilis</i> pyruvate decarboxylase promoter (P <i>pdc</i>), Strp ^R	This study
Strains	Description	Source
BL21(DE3)	F ⁻ <i>ompT hsdSB</i> (r _B ⁻ , m _B ⁻) <i>gal dcm</i> (DE3), a common expression host	Invitrogen

BH2	<i>E. coli</i> BL21(DE3) $\Delta xylA$ $\Delta tyrA$ $\Delta pheA$, an engineered strain with disrupted xylose catabolism, as well as tyrosine and phenylalanine pathways	(Zhang et al., 2015a)
XL10-Gold	<i>endA1 glnV44 recA1 thi-1 gyrA96 relA1 lac Hte</i> $\Delta(mcrA)183$ $\Delta(mcrCB-hsdSMR-mrr)173$ Tet^R $F'[\text{proAB}$ $\text{lacIqZ}\Delta\text{M15}$ $\text{Tn}10(\text{Tet}^R)$ Amy Cm^R], a strain with high transformation efficiency	Stratagene
BTH3	BH2 harboring pTE3 and pTD2	(Wang et al., 2019)
BTP1	BTH3 harboring pET21c	(Wang et al., 2019)
XYD	XL10-Gold harboring pET28a and pTY5	This study
BMC	BH2 harboring pTY2 and pTD2	This study
BMC2	BH2 harboring pTY2, pTD2 and pTC	This study
BLXC	BL21(DE3) harboring pTC	This study
BLXS	BL21(DE3) harboring pTS	This study
XTH	XL10-Gold harboring pTE3 and pTD3	This study
BTXC	BTH3 harboring pTC	This study
BTS	BTH3 harboring pTS	This study
BMS	BH2 harboring pTY2, pTD2 and pTS	This study
BTS1	BTH3 harboring pSE1	(Wang et al., 2019)
BMS1	BH2 harboring pTY2, pTD2 and pSE1	This study

488

489

490

491

492 **Reference**

493 1. Bayer, T. S., Widmaier, D. M., Temme, K., Mirsky, E. A., Santi, D. V., Voigt, C. A., 2009.
494 Synthesis of methyl halides from biomass using engineered microbes. *Journal of the American
495 Chemical Society.* 131, 6508-6515.

496 2. Burkovski, A., Krämer, R., 2002. Bacterial amino acid transport proteins: occurrence,
497 functions, and significance for biotechnological applications. *Applied microbiology and
498 biotechnology.* 58, 265-274.

499 3. Chen, T., Zhou, Y., Lu, Y., Zhang, H., 2019. Advances in heterologous biosynthesis of plant
500 and fungal natural products by modular co-culture engineering. *Biotechnology letters.* 41, 27-
501 34.

502 4. Clomburg, J. M., Gonzalez, R., 2013. Anaerobic fermentation of glycerol: a platform for
503 renewable fuels and chemicals. *Trends in biotechnology.* 31, 20-28.

504 5. Ganesan, V., Li, Z., Wang, X., Zhang, H., 2017. Heterologous biosynthesis of natural product
505 naringenin by co-culture engineering. *Synthetic and systems biotechnology.* 2, 236-242.

506 6. Gong, F., Yanofsky, C., 2001. Reproducing tna operon regulation in vitro in an S-30 system
507 tryptophan induction inhibits cleavage of TnaC peptidyl-tRNA. *Journal of Biological
508 Chemistry.* 276, 1974-1983.

509 7. Guo, X., Li, Z., Wang, X., Wang, J., Chala, J., Lu, Y., Zhang, H., 2019. *De novo* phenol
510 bioproduction from glucose using biosensor - assisted microbial co - culture engineering.
511 *Biotechnology and bioengineering.*

512 8. Jawed, K., Yazdani, S. S., Koffas, M. A., 2019. Advances in the development and application
513 of microbial consortia for metabolic engineering. *Metabolic Engineering Communications.*
514 e00095.

515 9. Jones, J. A., Vernacchio, V. R., Collins, S. M., Shirke, A. N., Xiu, Y., Englaender, J. A., Cress,
516 B. F., McCutcheon, C. C., Linhardt, R. J., Gross, R. A., 2017. Complete biosynthesis of
517 anthocyanins using *E. coli* polycultures. *MBio.* 8, e00621-17.

518 10. Jones, J. A., Wang, X., 2018. Use of bacterial co-cultures for the efficient production of
519 chemicals. *Current opinion in biotechnology.* 53, 33-38.

520 11. Kang, S., Kang, K., Lee, K., Back, K., 2007. Characterization of tryptamine 5-hydroxylase and
521 serotonin synthesis in rice plants. *Plant cell reports.* 26, 2009-2015.

522 12. Lee, S. J., Sim, G.-Y., Lee, Y., Kim, B.-G., Ahn, J.-H., 2017. Engineering of *Escherichia coli*
523 for the synthesis of N-hydroxycinnamoyl tryptamine and serotonin. *Journal of industrial*
524 *microbiology & biotechnology.* 44, 1551-1560.

525 13. Li, Z., Wang, X., Zhang, H., 2019. Balancing the non-linear rosmarinic acid biosynthetic
526 pathway by modular co-culture engineering. *Metabolic engineering.* 54, 1-11.

527 14. Liu, S.-D., Wu, Y.-N., Wang, T.-M., Zhang, C., Xing, X.-H., 2017. Maltose utilization as a
528 novel selection strategy for continuous evolution of microbes with enhanced metabolite
529 production. *ACS synthetic biology.* 6, 2326-2338.

530 15. Lv, Y., Qian, S., Du, G., Chen, J., Zhou, J., Xu, P., 2019. Coupling feedback genetic circuits
531 with growth phenotype for dynamic population control and intelligent bioproduction. UMBC
532 Faculty Collection.

533 16. Mahmood, Z. A., Ahmed, S. W., Azhar, I., Sualeh, M., Baig, M. T., Zoha, S., 2010.
534 BIOACTIVE ALKALOIDS PRODUCED BY FUNGI I. UPDATES ON ALKALOIDS
535 FROM THE SPECIES OF THE GENERA BOLETUS, FUSARIUM AND PSILOCYBE.
536 *Pakistan journal of pharmaceutical sciences.* 23.

537 17. Mattam, A. J., Clomburg, J. M., Gonzalez, R., Yazdani, S. S., 2013. Fermentation of glycerol
538 and production of valuable chemical and biofuel molecules. *Biotechnology letters*. 35, 831-
539 842.

540 18. Mora-Villalobos, J.-A., Zeng, A.-P., 2018. Synthetic pathways and processes for effective
541 production of 5-hydroxytryptophan and serotonin from glucose in *Escherichia coli*. *Journal of*
542 *biological engineering*. 12, 3.

543 19. Mousseau, D. D., 1993. Tryptamine: a metabolite of tryptophan implicated in various
544 neuropsychiatric disorders. *Metabolic brain disease*. 8, 1-44.

545 20. Niehaus, L., Boland, I., Liu, M., Chen, K., Fu, D., Henckel, C., Chaung, K., Miranda, S. E.,
546 Dyckman, S., Crum, M., 2019. Microbial coexistence through chemical-mediated interactions.
547 *Nature communications*. 10, 2052.

548 21. Park, S., Kang, K., Lee, S. W., Ahn, M.-J., Bae, J.-M., Back, K., 2011. Production of serotonin
549 by dual expression of tryptophan decarboxylase and tryptamine 5-hydroxylase in *Escherichia*
550 *coli*. *Applied microbiology and biotechnology*. 89, 1387-1394.

551 22. Pradima, J., Kulkarni, M. R., 2017. Review on enzymatic synthesis of value added products of
552 glycerol, a by-product derived from biodiesel production. *Resource-Efficient Technologies*. 3,
553 394-405.

554 23. Roell, G. W., Zha, J., Carr, R. R., Koffas, M. A., Fong, S. S., Tang, Y. J., 2019. Engineering
555 microbial consortia by division of labor. *Microbial cell factories*. 18, 35.

556 24. Røgkjær, P., Sarup-Lytzen, K., Nagy, M., Sommer, M. O. A., 2018. Synthetic addiction
557 extends the productive life time of engineered *Escherichia coli* populations. *Proceedings of the*
558 *National Academy of Sciences*. 115, 2347-2352.

559 25. Snoek, T., Romero-Suarez, D., Zhang, J., Ambri, F., Skjoedt, M. L., Sudarsan, S., Jensen, M.
560 K., Keasling, J. D., 2018. An orthogonal and pH-tunable sensor-selector for muconic acid
561 biosynthesis in yeast. *ACS synthetic biology*. 7, 995-1003.

562 26. Songstad, D. D., De Luca, V., Brisson, N., Kurz, W. G., Nessler, C. L., 1990. High levels of
563 tryptamine accumulation in transgenic tobacco expressing tryptophan decarboxylase. *Plant
564 physiology*. 94, 1410-1413.

565 27. Wang, X., Cabales, A., Li, Z., Zhang, H., 2019. Biosensor-assisted high performing cell
566 selection using an *E. coli* toxin/antitoxin system. *Biochemical engineering journal*. 144, 110-
567 118.

568 28. Xiao, Y., Bowen, C. H., Liu, D., Zhang, F., 2016. Exploiting nongenetic cell-to-cell variation
569 for enhanced biosynthesis. *Nature chemical biology*. 12, 339.

570 29. Yanofsky, C., Horn, V., Gollnick, P., 1991. Physiological studies of tryptophan transport and
571 tryptophanase operon induction in *Escherichia coli*. *Journal of bacteriology*. 173, 6009-6017.

572 30. Zhang, H., Li, Z., Pereira, B., Stephanopoulos, G., 2015a. Engineering *E. coli*-*E. coli*
573 cocultures for production of muconic acid from glycerol. *Microbial cell factories*. 14, 134.

574 31. Zhang, H., Pereira, B., Li, Z., Stephanopoulos, G., 2015b. Engineering *Escherichia coli*
575 coculture systems for the production of biochemical products. *Proceedings of the National
576 Academy of Sciences*. 112, 8266-8271.

577 32. Zhang, H., Stephanopoulos, G., 2016. Co-culture engineering for microbial biosynthesis of 3-
578 amino-benzoic acid in *Escherichia coli*. *Biotechnology journal*. 11, 981-987.

579 33. Zhang, H., Wang, X., 2016. Modular co-culture engineering, a new approach for metabolic
580 engineering. *Metabolic engineering*. 37, 114-121.

581 34. Zhou, Y., Li, Z., Wang, X., Zhang, H., 2019. Establishing microbial co-cultures for 3-
582 hydroxybenzoic acid biosynthesis on glycerol. *Engineering in Life Sciences*. 19, 389-395.

583